Broadband Phase Resolving Spectrum Analyzer Measurement for EMI Scanning Applications

Zongyi Chen[†1], Shubhankar Marathe[*2], Hamed Kajbaf[‡3], Stephan Frei[†4], David Pommerenke[*5]
[†] TU Dortmund University, Dortmund, Germany
[1]zongyi.chen,[4]stephan.frei@tu-dortmund.de
[*] EMC Laboratory, Missouri University of Science and Technology. Rolla, MO, USA
[2]skmcr4,[5]davidjp@mst.edu
[‡] Amber Precision Instruments, San Jose, CA, USA
[3]hamed@amberpi.com

***Abstract*— EMI scanning application requires phase and magnitude information for the creation of equivalent radiation models and for far-field prediction. Magnitude information can be obtained using rather an inexpensive spectrum analyzer (SA). Phase-resolving instruments such as vector network analyzers (VNAs) or oscilloscopes are very expensive for frequencies above 5 GHz. For this reason, this paper proposes a method that utilizes an SA for phase-resolved magnitude measurements. The basic principle is to measure the sum or difference of two signals for different phase shifts and deduct the phase from the effect difference of those measurements. The phase is retrieved using an optimization procedure. It is shown that the proposed approach can recover phase deviation within 20° when using six steps of variable attenuator control voltage for the test cases between 5 and 12 GHz.**

Keywords—EMI scanning, phase-resolved measurements, spectrum analyzer (SA)

I. INTRODUCTION

In many EMC applications, phase information of measured fields is desired in addition to conventional magnitude-only measurements. Among these applications, near-field scanning benefits strongly as source reconstruction or the application of Huygens surfaces becomes possible if phase-resolved field data is provided. Other applications of phase-resolved near-field measurement are near-field to far-field transformation (NFFF) **Error! Reference source not found.**, emission source localization methods such as emission source microscopy (ESM) [4], near-field analysis based on the surface equivalence principle (Huygens' Principle) [[1], [5], [6]], etc.

Several practical methods are proposed in the literature to measure or calculate phase from frequency domain or time domain measurements. The method used in [2] measures the field in time domain using an oscilloscope, converts the data to frequency domain using fast Fourier transform (FFT), and finally extracts the phase information by subtracting the measurement phase from the phase of a reference probe. The drawback of this method is the cost and lab availability of oscilloscopes for higher frequencies (above 4 GHz).

On the other hand, the method used in [4] and [7] measures the field in the frequency domain using a vector network analyzer (VNA). VNAs are precise instruments for measuring magnitude and phases. However, usually the VNAs measure the phase with respect to internal RF source of the instrument for S-parameter measurement. As proposed in [4], the tuned receiver mode of VNAs can be used for phase measurement with respect to an external source. The drawback of this method is poor image and spurious rejection of many VNAs in tuned receiver mode which leads to difficulties if the spectrum contains many signals, including pulsed and broadband signals other than the signal of interest.

Availability and low cost of spectrum analyzers (SAs) at very high frequencies makes them suitable for near field scanning. Another advantage is offered by different types of detectors, such as quasi-peak or average detectors which are required for EMI measurements. However, SAs are only able to resolve magnitude or I/Q components relative to its own signal source, which makes it unsuitable for EMI scanning if both phase and magnitude of field data are desired. This paper proposes a practical, broadband swept frequency method for magnitude and phase measurement using SA.

Usually, in phase-resolved scanning, one probe (field probe) is moved and a phase reference signal is taken from a fixed location, either via a second probe (reference probe) or by directly accessing a signal within the device under test (DUT) [1], [4]. In [8][9], a method is described that determines the phase from multiple SA measurements. In this method, a 0° hybrid coupler sums the field probe and the reference probe signals. To retrieve the phase, at least three sweeps are required. Each sweep uses a different configuration for the sum of the signals. However, the method fails to obtain useful phase information if the magnitude difference between the reference probe and the field probe signals is large. This is a result of using the magnitude change of vector additions at different phase angles. If the phase of the smaller signal is changed, the magnitude of the sum will change very little. Further, the method in [8][4] has been described for only single frequency application.

This paper discusses how to overcome both limitations, since the SA method allows phase measurements of many frequencies to be taken simultaneously and is less sensitive to differences in magnitude between the field probe and the reference probe signals. Similar to [8][9], the proposed method uses combinations of the field probe and the reference probe signals. However, the measurement is performed at different reference probe signal attenuation levels. In this way, it is ensured that for one measurement data set the field and the reference probe have similar magnitudes. This allows the phase to be resolved even if the field probe and reference probe signal amplitudes are very different. The SA method was tested using a comb generator to create signals from 5 to 12 GHz every 200

MHz and a voltage variable attenuator with a 30 dB adjustment range.

II. PRINCIPLES

Similar to [8][9], the field probe and the reference probe signals are combined using different phase shifts. The combination can be achieved by taking the sum and/or the difference. The analysis of the methods presented in **Error! Reference source not found.**-[8] showed that the SA method only works if the magnitudes of the field probe and reference probe signals are similar. To overcome this, a variable attenuator was added. If the combinations of the field probe and reference probe signals are measured multiple times (for example, at six attenuator settings) there will be an attenuator setting at which the magnitudes of the field probe and the reference probe are similar, providing that the field probe signal is very weak. If its magnitude is too weak, it is most likely not of interest for many EMI applications. For the verification of the concept given signals are used instead of probes. However, using signals from probes with sufficient low noise amplification is a straightforward change to the system, thus, only the phase resolving has been investigated for this paper.

Two implementations have been tested in this research:

I. Using the sum and difference for two different cable lengths in the reference branch, producing two different phase shifts (shown in **Error! Reference source not found.**).

II. Using only the sum for three different cable lengths in the reference branch, producing three different phase shifts (shown in **Error! Reference source not found.**).

Implementation II was developed to avoid the expensive broadband 180° hybrid.

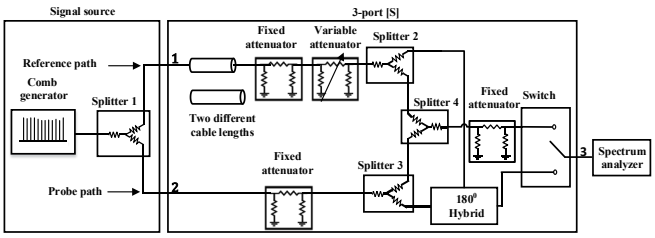

Fig. 1 Block diagram of Implementation I

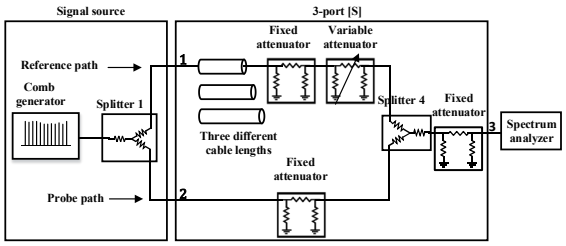

Fig. 2 Block diagram of Implementation II

In this experiment, six attenuation levels adjusted by voltage-controlled variable attenuator are used in both implementations, and each set-up is characterized by its 3-port S-parameters. The set-ups are as follows:

- Set-up I: six attenuator settings and two cables resulting in 12 S-parameter sets.
- Set-up II: six attenuator settings and three cables resulting in 18 S-parameter sets.

Fixed attenuators are used to improve the input match such that input reflections can be neglected. In a real scanning set-up, amplifiers would be in the probe and reference paths so additional loss of the attenuators would not diminish the system noise figure, and possible reflections between the amplifiers and the system would be expressed in the S-parameter set. For set-up I, switch has very good isolation, the multiple reflection between switch and SA can be neglected.

Set-up II simply replaced the expensive 180° hybrid coupler. Therefore, only the mathematical calculation is demonstrated for Set-up I. At each attenuator setting four sweeps were performed. Measured sum and difference of power were recorded for the shorter phase shift cable as $P_{meas\Sigma}$ and $P_{meas\Delta}$, respectively. Using a longer cable length (=phase shift), two more sweeps were carried out and the results are denoted by $P_{meas\Sigma\_s}$ and $P_{meas\Delta\_s}$.

Expressing the output signals by the S-parameters of the system leads to:

$$\begin{aligned}\left|b_{3\_meas\Sigma}\right|^2 &= |S_{31\Sigma}a_1+S_{32\Sigma}a_2|^2 \\ &= |S_{31\Sigma}|^2|a_1|^2 + |S_{32\Sigma}|^2|a_2|^2 + \\ 2|S_{31\Sigma}||a_1||S_{32\Sigma}||a_2|\,cos(\emptyset_{1\Sigma} - \emptyset_{3\Sigma} + \varphi)\end{aligned} \quad (1)$$

$$\begin{aligned}\left|b_{3\_meas\Delta}\right|^2 &= |S_{31\Delta}a_1+S_{32\Delta}a_2|^2 \\ &= |S_{31\Delta}|^2|a_1|^2 + |S_{32\Delta}|^2|a_2|^2 + \\ 2|S_{31\Delta}||a_1||S_{32\Delta}||a_2|\,cos(\emptyset_{1\Delta} - \emptyset_{3\Delta} + \varphi)\end{aligned} \quad (2)$$

$$\begin{aligned}\left|b_{3\_meas\Sigma\_s}\right|^2 &= \left|S_{31\Sigma\_s}a_1+S_{32\Sigma\_s}a_2\right|^2 \\ &= \left|S_{31\Sigma\_s}\right|^2|a_1|^2 + \left|S_{32\Sigma\_s}\right|^2|a_2|^2 + \\ 2\left|S_{31\Sigma\_s}\right||a_1|\left|S_{32\Sigma\_s}\right||a_2|\,cos\left(\emptyset_{1\Sigma\_s} - \emptyset_{3\Sigma\_s} + \varphi\right)\end{aligned} \quad (3)$$

$$\begin{aligned}\left|b_{3\_meas\Delta\_s}\right|^2 &= \left|S_{31\Delta\_s}a_1+S_{32\Delta\_s}a_2\right|^2 \\ &= \left|S_{31\Delta\_s}\right|^2|a_1|^2 + \left|S_{32\Delta\_s}\right|^2|a_2|^2 + \\ 2\left|S_{31\Delta\_s}\right||a_1|\left|S_{32\Delta\_s}\right||a_2|\,cos\left(\emptyset_{1\Delta\_s} - \emptyset_{3\Delta\_s} + \varphi\right)\end{aligned} \quad (4)$$

where $S_{31\Sigma}$, $S_{32\Sigma}$ are S-parameters measured if the system is configured to measure the sum $P_{meas\Sigma}$ using the shorter cable,

$S_{31\Sigma\_s}$, $S_{32\Sigma\_s}$ are S-parameters measured if the system is configured to measure the sum $P_{meas\Sigma\_s}$ using the longer cable,

$S_{31\Delta}$, $S_{32\Delta}$ are S-parameters measured if the system is configured to measure the sum $P_{meas\Delta}$ using the shorter cable,

$S_{31\Delta\_s}$, $S_{32\Delta\_s}$ are S-parameters measured if the system is configured to measure the sum $P_{meas\Delta\_s}$ using the longer cable,

$\emptyset_{1\Sigma}$ is the phase of $S_{31\Sigma}$, $\emptyset_{3\Sigma}$ is the phase of $S_{32\Sigma}$,
$\emptyset_{1\Delta}$ is the phase of $S_{31\Delta}$, $\emptyset_{3\Delta}$ is the phase of $S_{32\Delta}$,
$\emptyset_{1\Sigma\_s}$ is the phase of $S_{31\Sigma\_s}$, $\emptyset_{3\Sigma\_s}$ is the phase of $S_{32\Sigma\_s}$,
$\emptyset_{1\Delta\_s}$ is the phase of $S_{31\Delta\_s}$, $\emptyset_{3\Delta\_s}$ is the phase of $S_{32\Delta\_s}$,
φ is phase difference, $\varphi = \emptyset_{a2} - \emptyset_{a1}$.

The input parameters for equations **Error! Reference source not found.** through **Error! Reference source not found.** are $|a_1|$, $|a_2|$ and φ. Here, $|a_1|$ is the reference probe signal from a fixed location. It can be measured once before the scan. Thus, $|a_1|$ is known. The unknowns are $|a_2|$ and φ.

For solving these unknown parameters, an optimization algorithm is applied to $|a_2|$ and $\emptyset_{a2}, \emptyset_{a1}$. The optimization iteratively minimizes the error between a calculated SA power and the actually measured SA value. This requires a set of start values for $|a_2|$ and $\emptyset_{a2}, \emptyset_{a1}$, then the calculated power can be obtained using:

$$P_{calcu\Sigma} = \frac{1}{2}\left|b_{3\_start\Sigma}\right|^2 = \frac{1}{2}\left|S_{31\Sigma}a_{1\_start} + S_{32\Sigma}a_{2\_start}\right|^2 \quad (5)$$

$$P_{calcu\Delta} = \frac{1}{2}\left|b_{3_{start\Delta}}\right|^2 = \frac{1}{2}\left|S_{31\Delta}a_{1\_start} + S_{32\Delta}a_{2\_start}\right|^2 \quad (6)$$

$$P_{calcu\Sigma\_s} = \frac{1}{2}\left|b_{3_{start\Sigma\_s}}\right|^2 = \frac{1}{2}\left|S_{31\Sigma\_s}a_{1\_start} + S_{32\Sigma\_s}a_{2\_start}\right|^2 \quad (7)$$

$$P_{calcu\Delta\_s} = \frac{1}{2}\left|b_{3_{start\Delta\_s}}\right|^2 = \frac{1}{2}\left|S_{31\Delta\_s}a_{1\_start} + S_{32\Delta\_s}a_{2\_start}\right|^2 \quad (8)$$

Where $a_{1\_start} = |a_1|e^{j\emptyset_{a1\_start}}$
$a_{2\_start} = |a_{2\_start}|e^{j\emptyset_{a2\_start}}$

Similar to other optimization functions, the convergence and accuracy of the combined results highly depended on the definition of the error function value which is minimized. Here, the error function is defined in dB by:

$$Error_{total} = Error_{\Sigma} + Error_{\Delta} + Error_{\Sigma\_s} + Error_{\Delta\_s}$$

Where $Error_{\Sigma} = \left|P_{meas_{\Sigma}} - P_{calcu_{\Sigma}}\right|$,
$Error_{\Delta} = \left|P_{meas\Delta} - P_{calcu\Delta}\right|$,
$Error_{\Sigma\_s} = \left|P_{meas_{\Sigma\_s}} - P_{calcu_{\Sigma\_s}}\right|$, and
$Error_{\Delta\_s} = \left|P_{meas\Delta\_s} - P_{calcu\Delta\_s}\right|$.

A potential problem lies in reaching the local minima. This can be avoided by optimizing the start values, which may require testing multiple different start values and accepting the converged result which shows the lowest error value as the best estimate of the global minima. In its present optimized Matlab implementation, the optimization takes around 1 second.

III. Implementation

The first implementation is shown in a block diagram and a photo (**Error! Reference source not found.** and

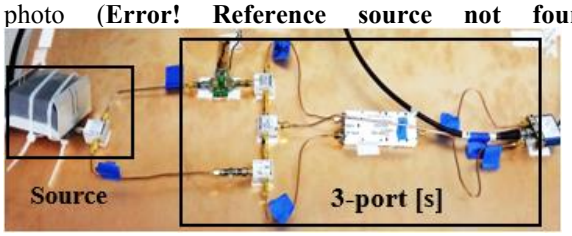

Fig. 3, respectively). The test signal was created using a comb generator and splitter 1, also shown in **Error! Reference source not found.**. A fixed attenuator of 6 dB was applied in the reference path and 20 dB in the probe path. A 5dB fixed attenuator was applied to output of splitter 4. The fixed attenuators were introduced to mitigate multiple reflections and to observe how the proposed method performed while having power level differences between the field probe and the reference probe signals.

The different attenuators in the probe and reference paths led to a 14 dB difference in the signal strength within the phase resolving system. Thus, the effect of the fixed attenuator was compensated for by a 14 dB setting of the variable attenuator, as shown in **Error! Reference source not found.** with a black line representing an attenuator control voltage equal to -1.5 V. It was expected that the lowest phase error was achieved at this setting. The measured 3-port system S-parameters are shown in Fig. 5. In this figure, S_{31} represents the reference path and S_{32} represents the probe path. The black box emphasizes the region where the magnitude of S_{31} is similar to S_{32}, which verifies the proper behavior of the variable attenuation settings.

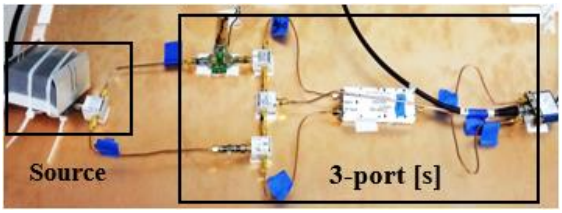

Fig. 3 Measurement setup for Implementation I

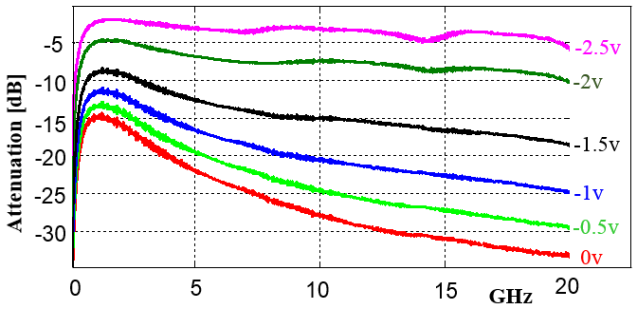

Fig. 4 Voltage-controlled variable attenuator

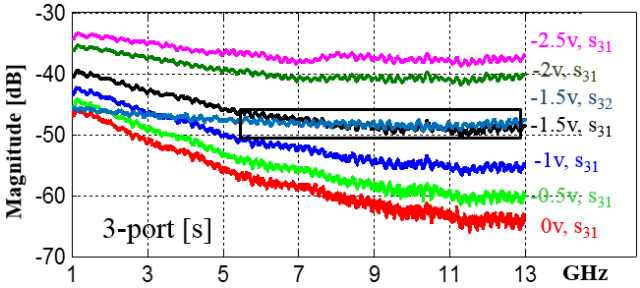

Fig. 5 System S-parameter corresponds to variable attenuator control voltages-Implementation I

A photo of Implementation II is shown in

Fig. 6. This set-up avoids the expensive hybrid coupler. A 180° hybrid coupler is identical to a 0° splitter and an inverter. One option is to build an inverter and use a splitter, and another is to introduce a third phase shift using cables. For a broadband method it is not possible to determine a cable length which will shift by 180° for all frequencies. As shown in Fig. 7, using three cables provides enough phase shift at every frequency investigated. For example, taking a frequency of 8 GHz, the phase difference between the reference signal ("ref") and cable I ("phase I") is 25°, and the phase difference between the reference signal ("ref") and cable II ("phase II") is 85°. This ensures no net effect would happen when observing measured powers. For Implementation II, fixed attenuators of 10 dB and 6 dB have been used, resulting in a different optimal variable attenuator setting—as shown in in

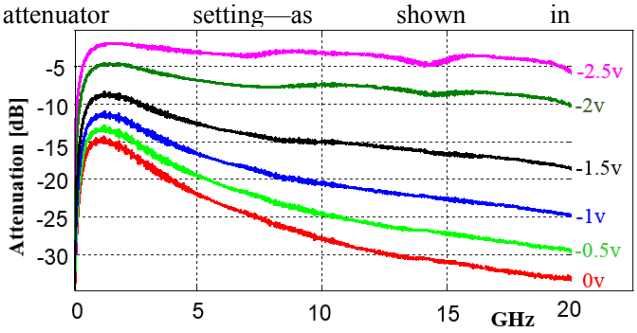

Fig. 4, an attenuator control voltage of -2 V leads to 6 dB. A 5dB fixed attenuator was applied to output of splitter 4 (shown in Fig. 2) so as to reduce possible multiple reflection between splitter 4 and SA.

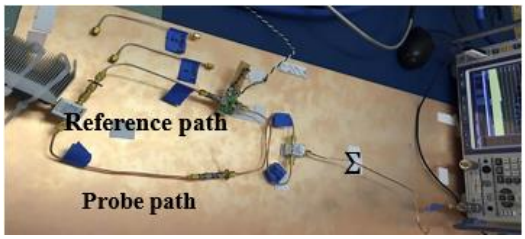

Fig. 6 Measurement setup for Implementation II

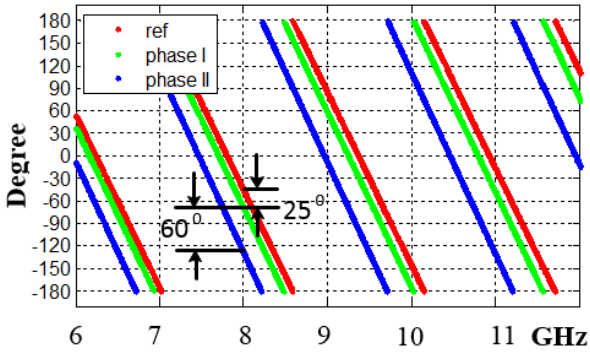

Fig. 7 Three phase shift cables–phase information

IV. Measurement Results

To validate the method, a broadband signal was created using an Omniyig comb generator. The source spectrum measured after splitter 1 is shown in

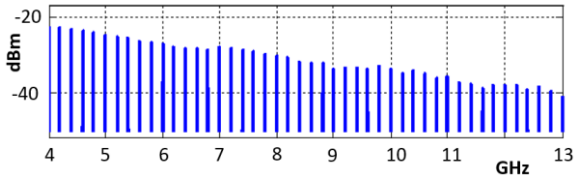

Fig. 8. The splitters are rated up to 12 GHz; for this reason the analysis was performed for the signals between 5 and 12 GHz.

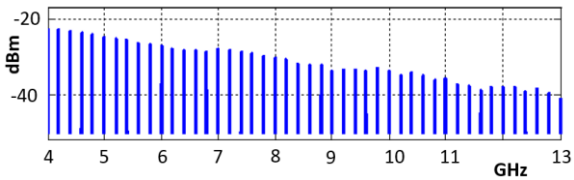

Fig. 8 Source power spectrum after splitter 1

Reference probe signal and field probe signal were obtained from the output signal of in-phase splitter 1, which means $|a_1|, |a_2|$ are known and $\varphi = 0°$. A known phase shift cable was then introduced to the reference path to create an out-of-phase reference probe signal and field probe signal. This allows comparison of the calculated phase and magnitudes to the real values of $|a_1|, |a_2|$ and φ. In this paper, Power "measured" means power directly measured by SA. Power "calculated" means power calculated using the measured S-parameters and the measured splitter 1 output values. Power "retrieved" means power retrieved through optimization algorithms and power "measured"

A. Measurement results–Implementation I

Due to the large amount of cables, splitters, and the usage of a voltage-controlled attenuator the system's S-parameters are error prone. We have observed variations from repeated dismounting, mounting, and S-parameter measurements in the range of +/- 0.5 dB. To test the effect of such errors and inaccuracies of the SA readings or time variations of the DUT emissions, simulations were performed that use the correct field probe and reference probe input signals and phases to calculate the power value that the SA would measure if the S-parameters were perfect. These calculated powers were then compared to the power measured by the SA.

As a representative example of the observed overall behavior, the data is shown in Fig. 9 for 8 GHz. Here, the dashed line with star denotes the magnitudes measured by the SA and the solid line with diamond denotes the values calculated using the measured S-parameters and the measured splitter 1 output values. The data match within ±0.5 dB. The black circle indicates a case in which the phase shifts add up such a way that the sum turns into a difference, which led to a minimum in the SA reading when the attenuator control voltage was -1.5 V. Such a cancellation point is rather sensitive to small phase and magnitude errors. The fact that a good match is achieved at such a cancellation point is an indicator for the robustness of the method.

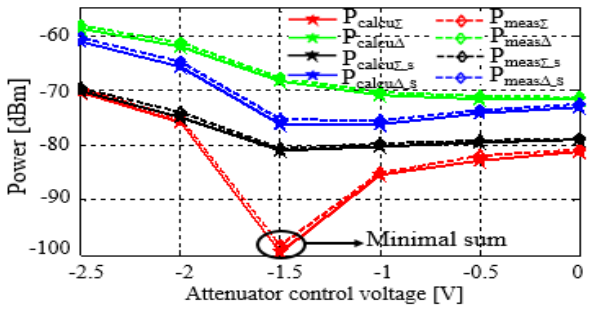

Fig. 9 Checking power measured compared with power calculated-implementation I

The reference probe was at a fixed location. Thus, the reference magnitude spectrum could be measured once before the scan. The reference magnitude spectrum was known. The optimization algorithm only needed to retrieve the field probe power, and phase difference between the reference probe and field probe signals. The correct phase difference between the reference probe and field probe signals of the test setup was 0°. As an in-phase splitter was used to create the field probe and reference probe signals (shown in **Error! Reference source not found.**, splitter 1), the retrieved field probe power should have been the same as the reference probe power. The results are shown in **Error! Reference source not found.** at 9 GHz and 11 GHz. For both frequencies, the retrieved field probe power shows a good agreement to the reference probe power among all attenuator settings. However, the retrieved phase shows more sensitivity to the attenuator setting. It was expected that the best phase recovery would be obtained at the attenuator setting, which leds to similar reference probe and field probe magnitudes at the splitter (shown in **Error! Reference source not found.**, splitter 4).

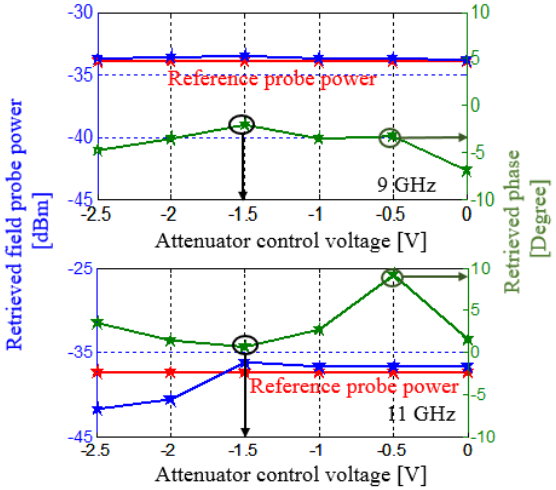

Fig. 10 indicates the same behavior is observed. At an attenuator control voltage of -1.5 V (the condition in which the variable attenuator produces a 14 dB attenuation to get similar reference probe and field probe signal levels), a phase error in the range of 10° was observed. This was most likely due to a sensitivity to an incorrect SA power measurement.

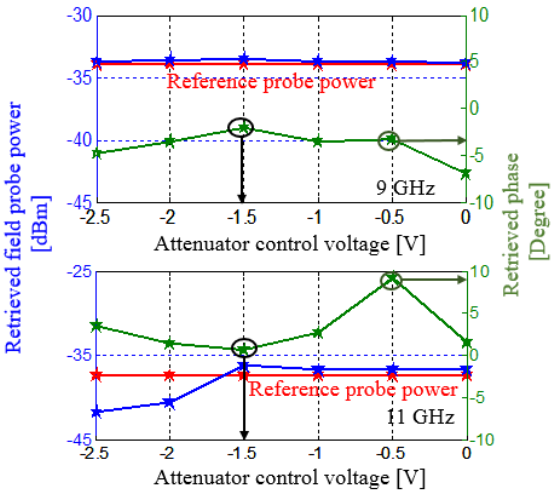

Fig. 10 Retrieved phase, probe power-Implementation I

The power measured by the SA is not an exact value. Errors can be introduced by time variation of the EMI signals of a DUT and by inaccuracies of the SA itself. To investigate the robustness of the phase and field probe power retrieval, the following numerical experiments have been conducted. Using the correct SA readings (four power measures for each variable attenuator setting, $P_{meas\,\Sigma}$, $P_{meas\Delta}$, $P_{meas\,\Sigma\_s}$, and $P_{meas\Delta\_s}$), a random distributed variation uniformly distributed at ±2.5 dB

was added to the correct values. The distributed values were then added to the optimization to identify the best fitting field probe powers and phase values. This was repeated 1000 times for different combinations of the distributed values. Each of the 1000 trials resulted in one best estimate of the field probe power and one estimate of the phase. Those results are illustrated in Fig. 11 for 7 GHz as histograms.

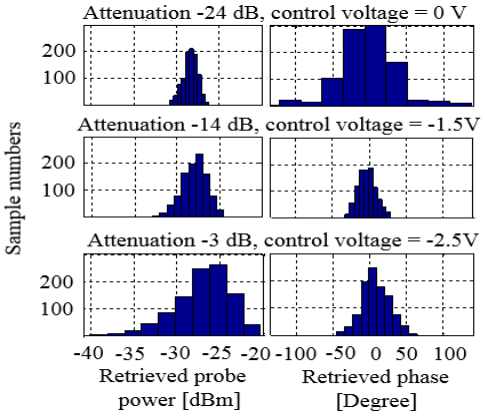

Fig. 11 Histogram of the retrieved field probe power (left) and the retrieved phase (right)

B. *Measurement results–Implementation II*

The second implementation used three different cable lengths for the phase shift instead of the hybrid coupler. First, an in-phase reference probe and field probe signal case was tested. Only the test set-up changed; the power capture and post-processing was similar to that of Implementation I. The retrieved field probe powers and retrieved phases at 7 GHz are shown in Fig. 12. The retrieved field probe powers followed the reference probe powers and a less than 1 dB deviation was observed. The retrieved phases were less than 20° when attenuator control voltage varied from -2.5 V to -1.5 V (best range).

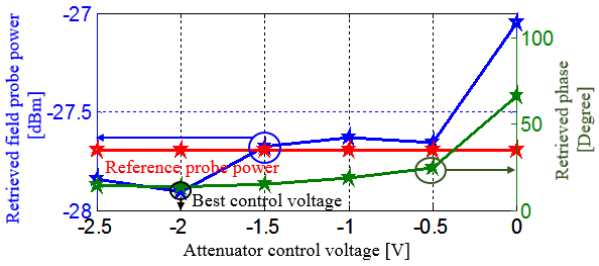

Furthermore, an out of phase reference probe and field probe signal case was also verified. An additional phase shift was introduced to the reference channel so that a phase difference could be detected between the reference probe and the field probe signals. The results of the configuration are shown in Fig. 13**Error! Reference source not found.**. The retrieved field probe power has less than 1 dB error for all attenuation settings. The phase was best retrieved at an attenuator setting of -2 V (= 7.5 dB attenuation). At that voltage, the field probe signal and the attenuated reference probe signal have about the same magnitude at splitter 4. Thus, the effect of adding different phase angles led to the largest magnitude changes. For an attenuator setting of 0 V (= 24 dB attenuation), the magnitude difference is too large such that the phase retrieval fails.

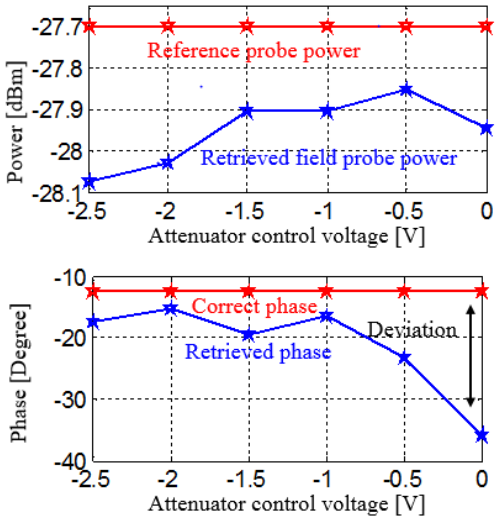

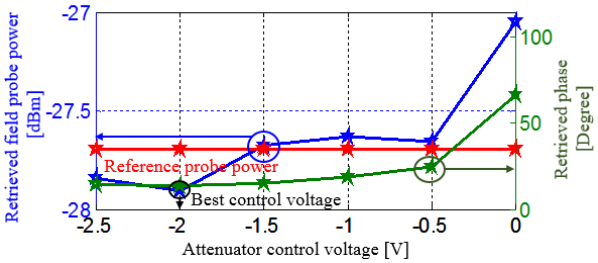

Fig. 12 Retrieved results of in-phase reference probe and field probe signals-Implementation II

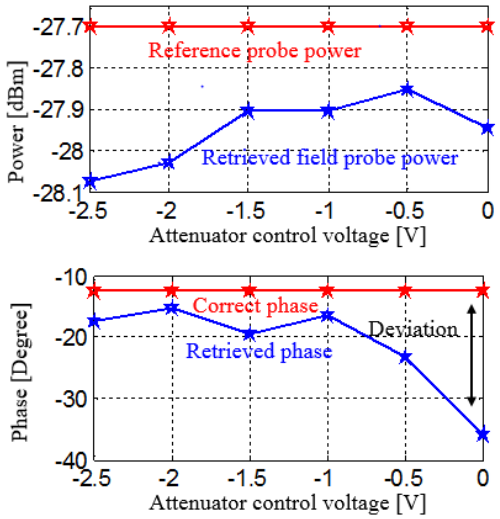

Fig. 13 Retrieved results of out of phase reference and field probe signal-Implementation II

V. DICUSSION

In this paper, the phase information of a broadband signal is recovered within ±20° of the actual phase value. As discussed in [6] and [10], far-field calculations based on the Huygens' box are rather insensitive to phase errors if the maximal signal is of interest. Since the magnitude errors are in the range of 1 dB, the proposed method could be practically used for this type of application

The analysis presented here shows two implementations for phase measurement setups. With controlling the reference signal level a good phase measurement accuracy could be reached. However, a set of limitations needs to be considered. Using different switchable attenuators, the frequency range of the hardware can be increased from a few MHz to 20 GHz, but the accuracy would suffer from the required phase shifts. If only one extra length cable and a 180° hybrid coupler is used as shown in **Error! Reference source not found.Error! Reference source not found.**, the selection of the cable length would be required on one side to have a reasonable phase change at the lowest frequency, but not to reach 360° at the highest frequency. If it would shift the phase by 360°, no net effect would be achieved. If the lowest phase shift is estimated to be 30° and the largest is estimated to be 300° then a 1:10 frequency range may be achievable.

The comb generator covered a range from -39 to -27 dBm between 5 and 12 GHz. The spectral components of the signals of interest usually also cover a limited amplitude range, as the lowest signals are generally of no interest from an EMI point of view. The range of the amplitudes that can be phase resolved depends on the attenuations used in the reference channel. A stepping of about 5 dB revealed good data. Much larger steps would reduce accuracy. Thus, to cover a range of 30 dB, six steps are needed resulting in 18 sweeps at each scan point (Implementation II) and 24 sweeps (Implementation I). We assume that the number of sweeps could be further reduced, but it will require more experience with the SA method. In summary, broadband phase-resolved scanning using an SA is possible, however, additional hardware is needed and the scan time increases.

VI. CONCLUSION

EMI scanning often requires phase- and magnitude-resolved field data. A broadband method to capture phase and magnitude data using an SA is discussed. Using a variable attenuator to match power levels of the reference probe and field probe signals can increase the phase measurement accuracy significantly. The presented implementation requires minimum 18 sweeps at each test point. Using 100 kHz resolution bandwidth and a sweep from 6 to 9 GHz and 30000 points a sweep time of 30ms was measured on an FSV-30 (Rhode & Schwarz) SA. Assuming 20ms for data transfer this leads to a scan time per point of about 2 seconds including 1 sec to move the probe. For lower RBW a list sweep (only measure frequencies of interest) is advisable to keep the sweep time acceptably low. In its present un-optimized Matlab implementation the optimization requires several seconds. With the investigated configurations phase was recovered within an error margin of about ±20°.

REFERENCES

[1] K. Kam, A. Radchenko, and D. Pommerenke, "On different methods to combine cable information into near-field data for far-field estimation," *in Proc. IEEE Int. Symp. Electromagn. Compat.,* pp. 294-300, August 2012.

[2] J. Zhang, K. W. Kam, J. Min, V.V. Khilkevich, D. Pommerenke, and J. Fan, "An effective method of probe calibration in phase resolved Near-field scanning for EMI application," *IEEE Trans. Instrum. Meas.,* vol. 62, no. 3, pp.648-658, March 2013.

[3] J. Zhang., Source reconstructions for IC radiated emissions based on magnitude-only near-field scanning, Ph.D. dissertation, EMC lab, Missouri S&T., Rolla, MO, USA, 2013.

[4] P. Maheshwari,V. Khilkevich, D. Pommerenke, H. Kajbaf, and J. Min, "Application of emission source microscopy technique to EMI source localization above 5 GHz," *IEEE Int. Symp. Electromagn. Compat.,* pp. 7-11, August 2014.

[5] X. Gao, J. Fan, Y. Zhang, H, Kajbaf, and D. Pommerenke, "Far-field prediction using only magnetic near-field scanning for EMI test," *IEEE Trans. Electromagn. Compat.,* vol. 56, no. 6, pp. 1335-1343, December 2014.

[6] M. Sorensen, O. Franek, G. Pedersen, A. Radchenko, K. Kam, and D. Pommerenke, "Estimate on the uncertainty of predicting radiated emission from Near-field scan caused by insufficient or inaccurate Near-field data," *IEEE Int. Symp. Electromagn. Compat.,* pp. 1-6, September 2012.

[7] A. Ramanujan, H. Shall, Z. Riah, F. Lafon, and M. Kadi, "From complex near-field measurements to radiated emissions modelling of electronic equipments," *IEEE Int. Symp. Electromagn. Compat.,* pp. 97-101, September 2014

[8] Y. Vives , C. Arcambal , A. Louis , F. de Daran, P. Eudeline, and B. Mazari, "Modeling magnetic radiations of electronic circuits using near-field scanning method," *IEEE Trans. Electromagn. Compat.,* vol. 49, no. 2, pp. 391-400, May 2007.

[9] Gilabert, Y. V. Modélisation des émissions rayonnées de composants électroniques. Ph.D. dissertation, Université de Rouen, 2007.

[10] A. Radchenko, J. Zhang, K. Kam, and D. Pommerenke, "Numerical evaluation of near-field to far-field transformation robustness for EMC," *IEEE Int. Symp. Electromagn. Compat.,* pp. 605-611, August 2012.